

# Optimal positioning of robot arms inside the abdominal cavity in pediatric surgery

Graphical User Interface for robotic trocar  
placement & the design of a 3D trocar  
placement tool and phantom.

---

Anna Ooms, s1540807, 12-08-21

2<sup>nd</sup> year Master Technical Medicine: Imaging & Intervention, internship  
nr.4.

## **Supervisors:**

Prof. E.C.J. Consten  
Dr. J. Sikorski  
Prof. S. Misra  
Dr. J.L.M. Bruggink  
Drs. R.H.J. de Kleine

Medical, Meander MC  
Technical, University of Twente  
Technical, University of Twente  
Medical, UMCG  
Medical, UMCG

## ABSTRACT

The success rate of the da Vinci Xi robot depends on the port placements, in which the manufacturer recommends a minimum distance of 6-8cm between each trocar. Achieving these distances is challenging for the University Medical Centre Groningen (UMCG) who operates young pediatric patients with choledochal malformation. The small pediatric abdomen compared to the robotic arms use increases the collision chance, which can cause injuries. Therefore, this research studies the optimal positioning of robot arms in pediatric abdominal surgeries. Two easy-to-use graphical user interfaces (GUIs) were designed in MATLAB (R2021a), which enabled to involve the surgeon's decision-making in trocar placement. The GUIs were used to compare the results of an integrated kinematic robot model for a straight-line to semi-circular port placement by integrating inverse kinematic solvers of previous work. Following from the GUIs were the design of a trocar placement tool in Materialise 3-Matic to mark the selected trocar locations of the GUI onto the patient's abdomen to bridge the graphic models with the operating room. Finally, this research designed a 3D phantom (Materialise 3-Matic) based on the torso of a segmented young child's abdomen. The semi-circular trocar placements resulted in less overlapping of external volumes of the kinematic robot and therefore indicated less collision chance. Furthermore, a design protocol was created for future use of the 3D trocar tool and phantom. This study recommends is recommended setting up future phantom studies to clinically validate the kinematic model and the trocar placement tool safely.

**Keywords**—da Vinci XI, Kinematics, Pediatric surgery, Port placement

## 1. Introduction

Image-guided laparoscopic surgery enables the performance of minimally invasive procedures and offers increased accuracy and safety for surgeons [1]. However, disadvantages of the laparoscopic procedures are the restricted range of motion, the two-dimensional (2D) vision, and the poor ergonomics positioning of the surgeon [2]. Therefore, in the past years, the Da Vinci robot (Intuitive Surgical, Mountain View, CA, United States) has been widely adopted to overcome these limitations and significantly improves the visualization and dexterity by the use of advanced equipment [2], [3]. Though, one major drawback of the robot is the high purchase costs [2].

Robotic surgery can provide care to complex minimal procedures and is even usable in pediatric surgery [4]. However, the challenge in pediatric robotic surgery lies in avoiding collision because of the size of the four robot arms in contrast with the patient's body [5]. The University Medical Centre Groningen (UMCG) at Groningen, the Netherlands, uses the da Vinci Xi robot in pediatric choledochal malformation surgery about five to six times a year. Choledochal malformations (also known as choledochal cysts) are congenital dilatations of the biliary tree, which are primary diagnosed in children [6]. They are treated by resecting the affected biliary tissue and creating either the Roux Y hepaticojejunostomy (most often preferred) or hepaticoduodenostomy [7].

During robotic surgery, the most critical issue is determining the placement of the ports and poses of the surgical robot [8]. Fig. 1 shows an example of the da Vinci Xi port placement in adult upper abdominal robotic surgery [9]. The ports are placed here in a straight line perpendicular to the target anatomy [9]. Before the port placement, the abdomen is insufflated to create a so-called

pneumoperitoneum. This allows more room and sight of the target organ for the surgeon. The pneumoperitoneum pressure ranges between 8 to 12 mmHg in children with a flow rate of 1 L/min [10]. The pediatric choledochal malformation surgery starts with an abdominal incision to place an Alexis laparoscopic system before the camera port is inserted [11]. In adult surgery, the camera port (port 3) is directly inserted into the umbilicus port. Under direct vision of the camera, the remaining three 8mm trocars are placed.

In contrast with the adult abdomen, there is no standardized way to place the trocars in pediatric choledochal malformation surgery. The manufacturer recommends a minimum distance of 8 cm to the target organ and 6-8 cm between each trocar to allow free movement of the da Vinci Xi robot, which is challenging in the small pediatric abdomen [12], [13]. However, if the distance of the port placement is too small, the arms have a higher chance of collision, which can cause injuries [14]. Therefore, it is important to gain more insight into the optimal positioning of the robot arms in pediatric abdominal surgery.

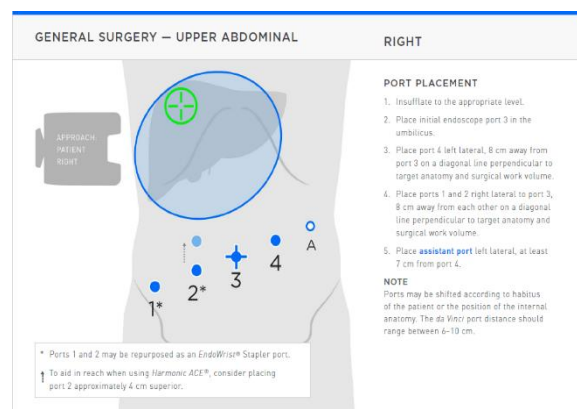


Fig. 1. Port placement of the da Vinci Xi robot in adult upper abdominal robotic surgery. Source: Stricko et al. (2018)

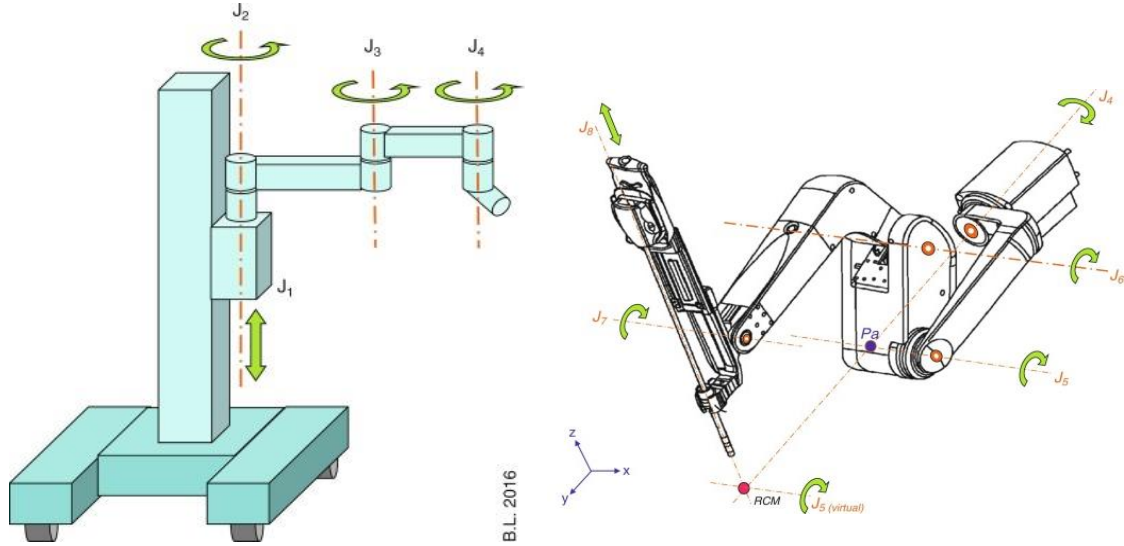


Fig. 2. Schematic overview of the movements of the da Vinci robot system. The first four arms of the robot are locked once the arm is correctly positioned (left panel) the remaining outer arms are actively retracted during surgery (right panel). Source: Lombard, (2016).

Previous studies about port optimization in pediatric surgery have designed a kinematic model of the robot to simulate the movements using generalized inversed kinematic (GIK) solvers [15], [16]. The movements of the da Vinci robot are schematically visualized in Fig. 2 [17]. The da Vinci robot system replicates the human wrist-like movements (pitch, yaw, and roll) and is capable of seven degrees of freedom (DOF) [18]. It either consists of rotation joints (revolute) or sliding joints (prismatic) [19].

The kinematic model of the previous work was described by the Denavit-Hartenberg (DH) convention, which means that each joint (Fig. 2) has its XYZ coordinate system [3]. The revolute joints rotate around its z-axis, and the prismatic joints translate around its z-axis [20]. The joints are first linked to each other by the translation and rotation of the x-axis and then by the translation and rotation of the z-axis [3]. Therefore, the origin of the following joints will not be in the center of the joint, but in the open space. Furthermore, the four transformation parameters include [20]:

- $d$  – Depth, which is the displacement along the previous joint's z-axis.
- $\theta$  – Rotation about the previous joint's z-axis to align with the x-axis.
- $r$  – Radius of the previous z to the new origin
- $\alpha$  – Rotation about the current joint's x-axis. If the z-axes are parallel, then  $\alpha=0$

Besides the kinematic model, other previous studies have designed a segmented patient model containing a pneumoperitoneum defined as a half ellipsoid point cloud [21], [22]. A schematic overview of the previous studies about port optimization is visualized in Fig. 3. Although promising progress was made in previous research,

the connection with practical implementation was lacking. For instance, the port coordinates for the kinematic model were set randomly. In addition, there was no translation between the models to the surgeons and operating room. Also, the kinematic model needs further improvement because the GIK solver sometimes led to unrealistic stretched arms [15]. Finally, the kinematic models are not clinically validated yet. Therefore, this research aims to overcome these limitations by improving the kinematic model and the design of a graphical user interface (GUI) to involve the surgeons in the trocar placement decision. To translate the results of the GUI to the operation room, this research aimed to design a 3D printed trocar placement tool based on the chosen trocar locations of the GUI. The trocar tool can be used to mark the chosen trocar locations pre-operatively onto the patient's abdomen. The final objective involved the clinical validation of the kinematic model, by aiming to design a phantom of a pediatric abdomen.

## 2. Methods

### 2.1 Graphical User Interface I

A trocar placement GUI was designed in MATLAB (R2021a, MathWorks INC., US), using the Robotics System Toolbox, based on a trocar placement tool GUI of previous research [21]. Several mouse-click buttons were designed into the GUI, allowing the surgeon to make the decision where the trocars should be placed in the patient's abdomen.

First, mouse click buttons were designed in the GUI that gives the user two options. Either the user can load in segmented patient data (STL file) or load in a patient surface patch model. The surface patch model consisted of ellipsoids, in which the abdominal ellipsoid was designed based

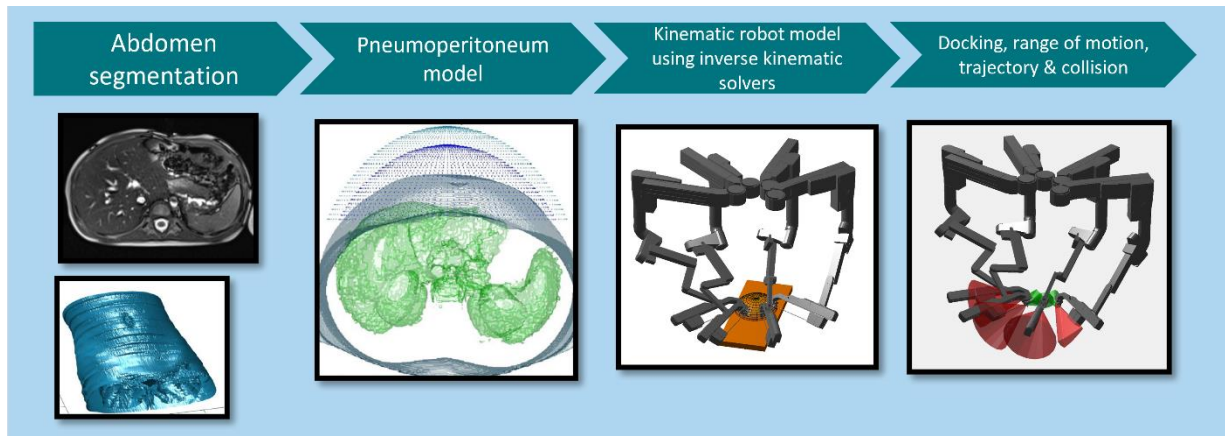


Fig. 3. Schematic overview of previous research about optimized port placement of the da Vinci Xi robot in pediatric surgery. First a patient model was designed from segmented CT & MRI data. A pneumoperitoneum was added to the model as a half ellipsoid point cloud. Next a kinematic model of the da Vinci robot was designed to simulate the movements of the robot. Using generalized inverse kinematic (GIK) solvers, the docking procedure and realized trajectories were simulated in which the range of motion was expressed as cone shaped volumes. Source: Pruijssers, (2021)

on the torso size of a segmented young child (see Fig. 4). The anatomical structures of the umbilicus and sternum were marked on the surface patch model by a black cross and the letters 'U' and 'S'. In addition, a green target dot was added located at the upper right abdomen. A rectangular surface patch was added, representing the patient table. The GUI allowed rotation of the loaded patient figures in any direction. Nevertheless, a specific XY-plane rotation button was added to visualize the patient directly in front of the user.

What followed was designing the placement of trocars at the desired location of the patient model. Four designed buttons with each a distinctive color and number represented a robotic arm. The trocar visualization was designed as an 8mm cylinder containing the same colors as the trocar buttons. The GUI also allowed the user to move each individual trocar after placement if the user is not satisfied with its chosen location. This was designed by deleting the trocar cylinder after

pressing the matching button again. In addition, a measurement tool was designed above the axes of the figure, which indicated the distance between each placed trocar. If the trocars were placed within a distance  $< 3\text{mm}$ , the measurement turned into a red 'warning' sign.

After the trocar placement buttons, a button was added that converted the decided trocar placement coordinates into the integrated GIK solver calculations of previous research [15], [16]. The GIK randomly solved the docking poses of the robot arms until no collision was detected using the trocar placement coordinates as port location constraints and the green target dot as an aiming constraint. An adjustment in the kinematic model was made to prevent unrealistic arm positions by setting the angle limit of joint nr. 8 to a range of  $45^\circ$  to  $180^\circ$  (instead of  $0^\circ$  to  $180^\circ$ ).

Besides the docking, another integrated GIK solver calculated the collision with the patient and table while each arm followed a circular trajectory with the tip of the tool [15]. This was followed by the calculation of the instrument reach of the last external link and internal part, expressed as cone shaped volumes.

Because these calculations took a while, a waiting text was implemented, which tells when the user is allowed to press the 'show results' button. This button opens a second GUI that will be further described in the next section.

## 2.2 Graphical User Interface II

This section describes the design of the second GUI in MATLAB (R2021a), using the Robotics System Toolbox. The GUI consisted again of easy-to-use mouse click buttons, in which each button was designed to load in a figure that presents a result of the kinematic robot model by the GIK solvers. Each of the results was presented together with the surface patch patient model.

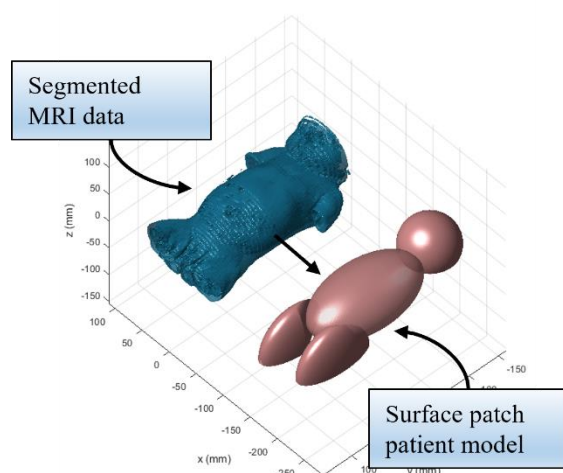


Fig. 4. Loaded in segmented MRI data of a segmented young child (left) and the same patient model as surface patch (right) made from ellipsoids. The torso ellipsoid equals the size of the child's body.



Another feature was constructed in this GUI, which was the graphic design of the 3D printed trocar placement tool. Two trocar tools were designed. Both designs consisted of drawn pentagon shapes at the location of each chosen trocar coordinate of GUI I. The pentagon shapes were connected by drawn triangular prisms. If one of the trocar coordinates were located at the umbilicus, the prisms were connected one by one from trocar 1 to 2, 2 to 3, etc. If not, a fifth pentagon shape was drawn at the coordinate of the umbilicus, to which all the connecting triangular prism were directed, creating a star-shaped tool. In both designs, an additional vertical prism and pentagon on top of the umbilicus were added to point out the direction of the tool during placement at the abdomen. The trocar tool designs were saved as STL files when pressing the button in the GUI. In addition, the abdominal ellipsoid of the surface patient model was also saved as an STL file, as a base for the design of a phantom.

### 2.3 Trocar placement comparison

This research also compared the outcome of the kinematic model for different trocar placements using the GUIs. The first trocar placement was placed in a straight line (Fig. 1) according to surgeons of the UMCG and the da Vinci Xi clinical specialty guide [9]. The second setup was placed in a semi-circular line to investigate which trocar placement gave the optimal robot arm positioning.

### 2.4 Completion of the 3D phantom model & trocar tool design.

For the completion of the 3D phantom and trocar placement tool, the STL files containing the trocar placement tool shapes and phantom were imported in the software program Materialise 3-Matic (Materialise, Leuven, Belgium).

The phantom was given holes at the coordinates of the chosen trocars of GUI I for the use of the robot arms, by subtracting the trocar pentagons files from the abdomen mesh. Also, a large hole was dissected at the back of the phantom for future implementation of anatomical structures within the phantom. For the trocar placement tools, the loose pentagon and prism shapes were merged to create one solid object.

Both the phantom and tools were given an external thickness of 3mm to generate firmness and were exported again STL files. The completion steps of the 3D phantom and trocar placement tool in Materialise 3-Matic were documented step by step in a design protocol.

## 3. Results

### 3.1 Trocar placement tool (GUI I)

Fig. 5 shows the starting screen when opening GUI I. The GUI fits the whole screen of the user and presents the mouse-click buttons on the left side. The circles which contain the capital letters in Fig 5 are not shown during the use of the GUI and were added for the following explanation of the GUI:

- A. Allows the user to load in an STL files containing segmented patient data.
- B. Opens a figure, containing a patient's surface patch model based on the segmented young child with a patient table.
- C. After pressing either A or B, the axis of the figure rotates to the XY plane.
- D. Trocar placement buttons, each button has a different color and number representing each robot arm. After clicking a button, the trocar can be placed on the patient model and appears as a cylinder. Clicking again on the same button after placement, allows the user to move the placed trocar cylinder.
- E. Starts the calculations of the GIK solvers with the coordinates of the placed trocars. When pressing the button, a waiting text appears (Fig. 11 Appendix A)
- F. Closes GUI I and opens GUI II.
- G. Opens a help text (Fig. 12 Appendix A)

Turning now to Fig. 6 which shows the screen of GUI I after finish clicking B. C. and D. The blue text rectangles and black arrows in Fig. 6 were not shown during the use of the GUI and were added in this figure as an additional explanation. As seen on the patient model, the umbilicus and sternum were marked by a black cross, and the target point of the robot was indicated by the green dot.

The trocars were placed here in the straight line as seen by the colored cylinders which corresponded with the colors of the 'Trocar ..' buttons. Above the axes of the patient model, the distance between the last-placed trocar nr. and the trocar nr. -1 appeared. In this fig. the distance between trocar 1-2 is shown, indicated that the last placed trocar was trocar nr. 2.

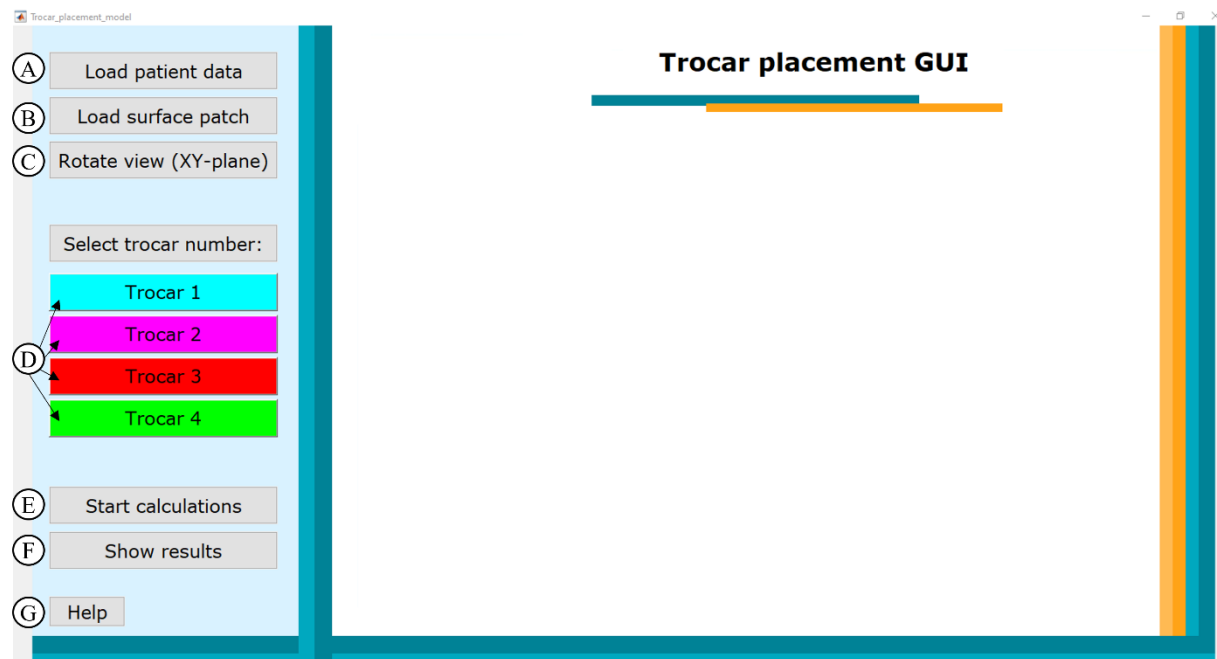


Fig. 6. Start screen of the trocar placement Graphical User Interface (GUI) in MATLAB (2021a) containing mouse-click buttons on the left side of the screen: A) Loads in segmented patient data as STL file. B) Loads a surface patch based on the segmentation of a young child. C) Rotates the loaded patient figure to the XY-plane. D) Trocar placement buttons allowing the user to choose the trocar location on the patient model after pressing. E) Starts two generalized inverse kinematic (GIK) solvers for kinematic robot model calculations. F) Opens another GUI to present the results of the GIK solvers. G) Help button, showing a screen with explanation text about the use of the GUI.

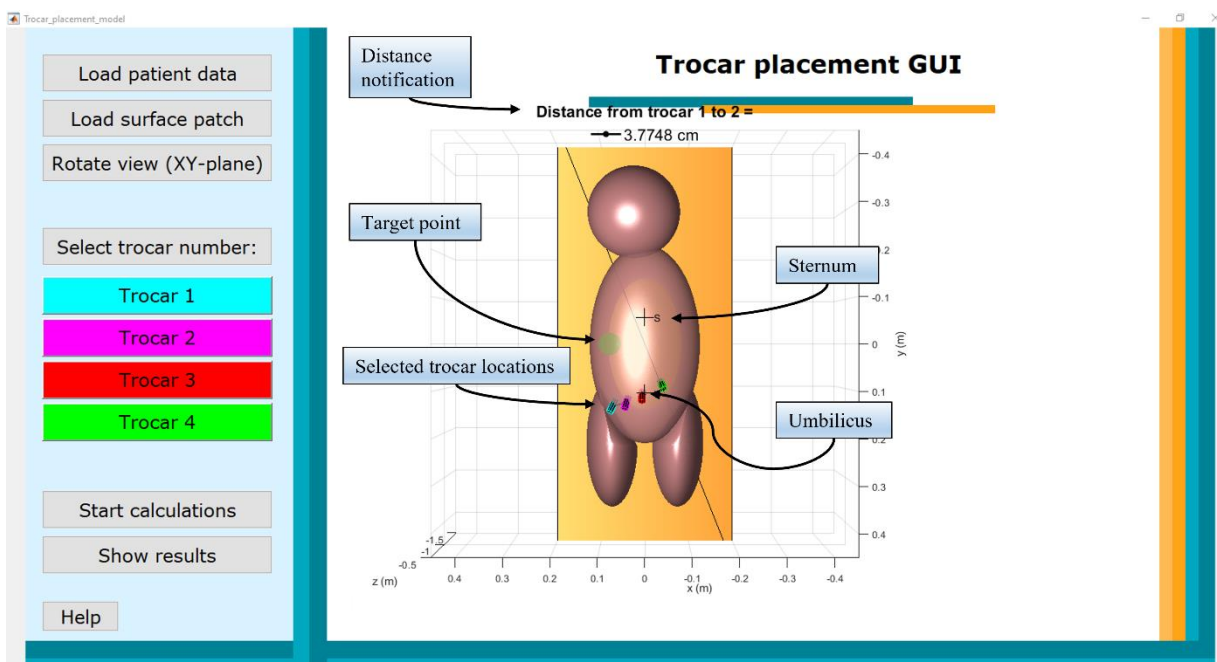


Fig. 5. Screen of the trocar placement Graphical User Interface (GUI) in MATLAB (R2021a) after loading in a surface patch patient model and table with the 'load surface patch' button. The sternum and umbilicus are marked with a black cross and the target point as green dot. Note the selected trocar locations, which appear as colored cylinders that are identical to the corresponding 'Trocar...' buttons. The distance notification on top of the figure informs the user about the distance between the last placed trocar (nr.) and trocar (nr. -1).

### 3.2 GIK solver Results (GUI II)

Fig. 7 shows the starting screen of GUI II, which opens after the ‘show results’ button of GUI I (Fig 5A). The layout of this GUI was similar to the previous GUI. Again, the circles that contain the capital letters in Fig. 7 were added for explanation and were not shown during the use of the GUI:

- A. Re-opens GUI I to look at the placed trocar locations, or to let the user make adjustments.
- B. Opens a figure to load in the patient surface patch with the design of the trocar placement tool. Fig. 13 Appendix B shows an example of the screen when pushing the button. The heptagons were given the same colors as the earlier placed trocar for clearance. The third trocar was located at the umbilicus and therefore, the vertical direction prism was placed on top of the third heptagon.
- C. Opens a figure to show the results of the docking GIK solver. As seen by the two blue-colored buttons, the user was given the option to visualize the docking results with only the joint frames (left button) of the robot arms or to visualize the docking result with visualization of the robot arms (right button).
- D. Opens a figure to show the results of the docked robot arms with their occupied volume after a circular trajectory movement of the last external link. The bottom left screen of Fig. 8 shows the result after clicking D. The red cones indicate the external volume of the arms and the internal part of the tool is shown in green.
- E. Opens a figure to show the same occupied volume results as D, but without the visualization of the robot arms.
- F. Opens a figure that shows the circular trajectories of the end tip of each robot arm (see the bottom right screen of Fig. 8).
- G. As seen in Fig. 7 four colored buttons represent each robot arm similar to in GUI I. Clicking on a number will open a figure with the representing robot arm and shows the realized trajectory with its robot arm tool deviation. (see Fig. 15 of Appendix B). The most deviation of the realized trajectory was caused by robot arm nr.1. Furthermore, robot arms 3 & 4 collide the most with the patient or table, which is indicated by the letter ‘c’.
- H. Opens a help text (Fig. 14 Appendix B)

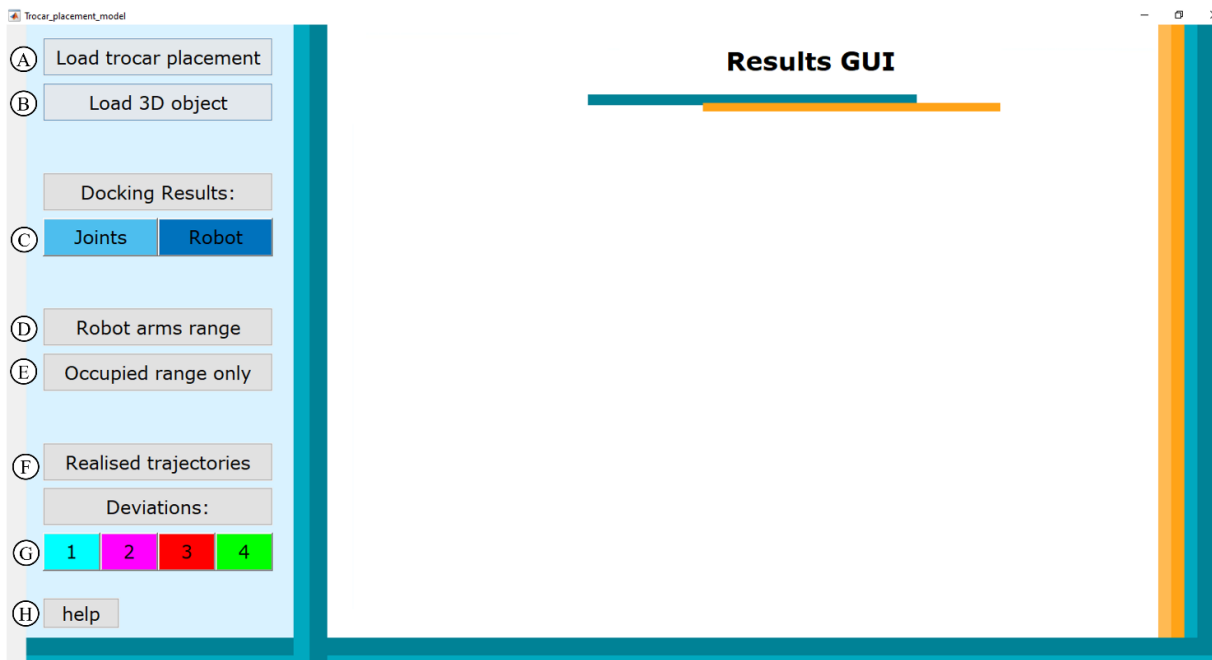


Fig. 7. Start screen of the results Graphical User Interface (GUI) in MATLAB (2021a) of the kinematic robot model after integration of the generalized inverse kinematic (GIK) solver, using the coordinates of the trocar placement GUI. The mouse-click buttons on the left side of the screen opens a figure showing: A) Loads in the trocar placement GUI with the previously placed trocars. B) Loads a graphic design of a 3D trocar placement tool. C) Loads in the patient model with the docking results of the robot arms with either showing only the joints, or with the visualization of the robot arms. D) Showing the visualization of the robot arms with their occupied volume after a circular trajectory movement of the last external link. E) Showing the same occupied volumes as in figure D) without the visualization of the robot arms. F) Shows the circular trajectories of each arm. G) Realized trajectory deviation of each individual robot arm. H) Opens the help text.

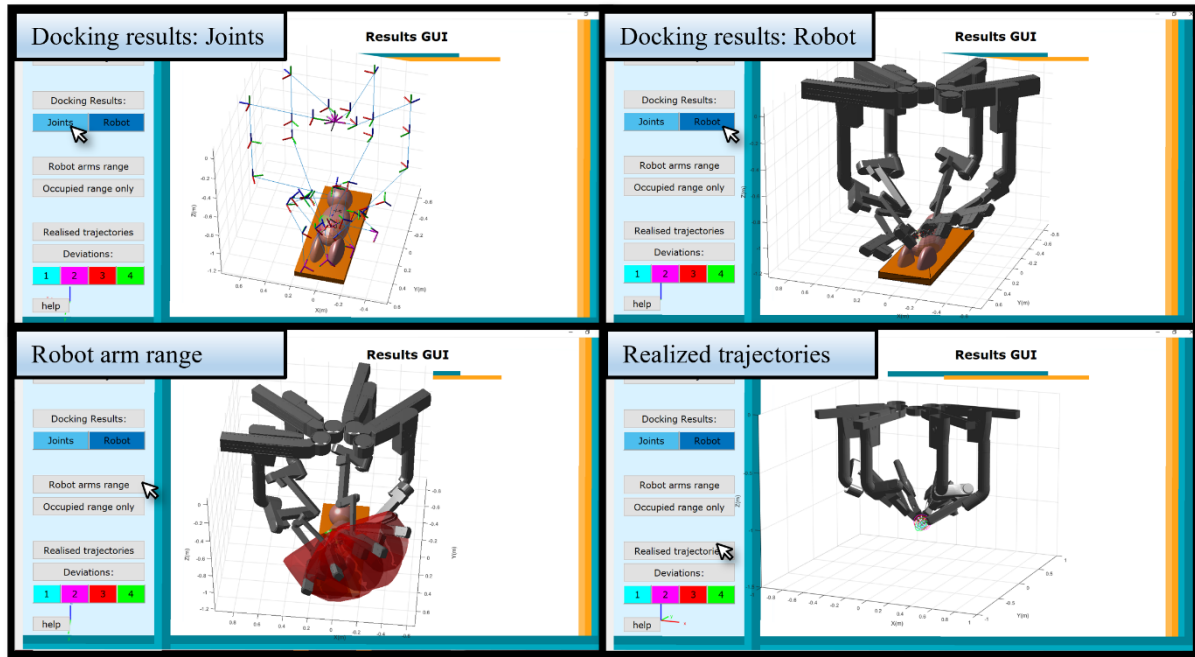


Fig. 8. Four different screens of the Graphical User Interface (GUI) in MATLAB (2021a) of the kinematic robot model after integration of the generalized inverse kinematic (GIK) solver. Each screen appears after clicking one of the buttons on the left side of each screen, the mouse cursor in each screen points which button is clicked. Upper left) The GIK solver docking result with visualization of the joints of the robot arms. Upper right) The GIK solver docking result with visualization of the robot arms. Bottom left) Occupied volume during trajectory of the last external link in red and internal part of the tool in green. Bottom right) Realized trajectories of the end tip of each robot arm.

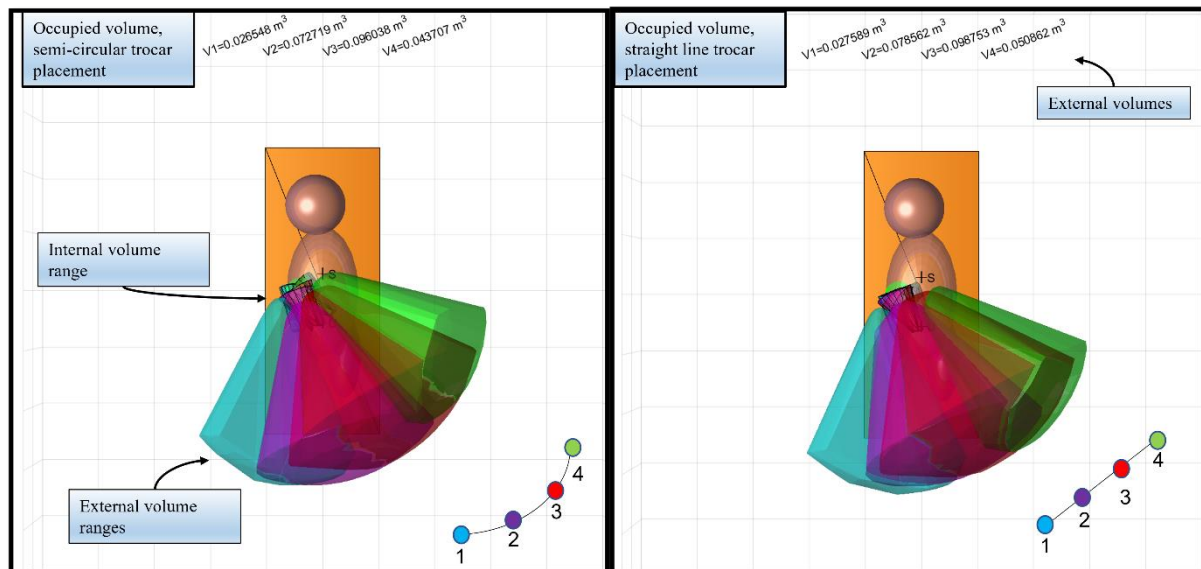


Fig 9. Comparison of the occupied volumes during trajectory of the last external link after a semicircular line (left panel) and straight (right panel) trocar placement. The internal volume ranges are indicated by the black edges around the cones. The external volume ranges are besides the colored cones, visible expressed in m3 above the figure. The drawing in the right corner indicates how the trocar were placed. Note that the semi-circular trocar placement has less overlapping between the external and internal volumes. However, the straight-line placement has larger occupied external volumes.



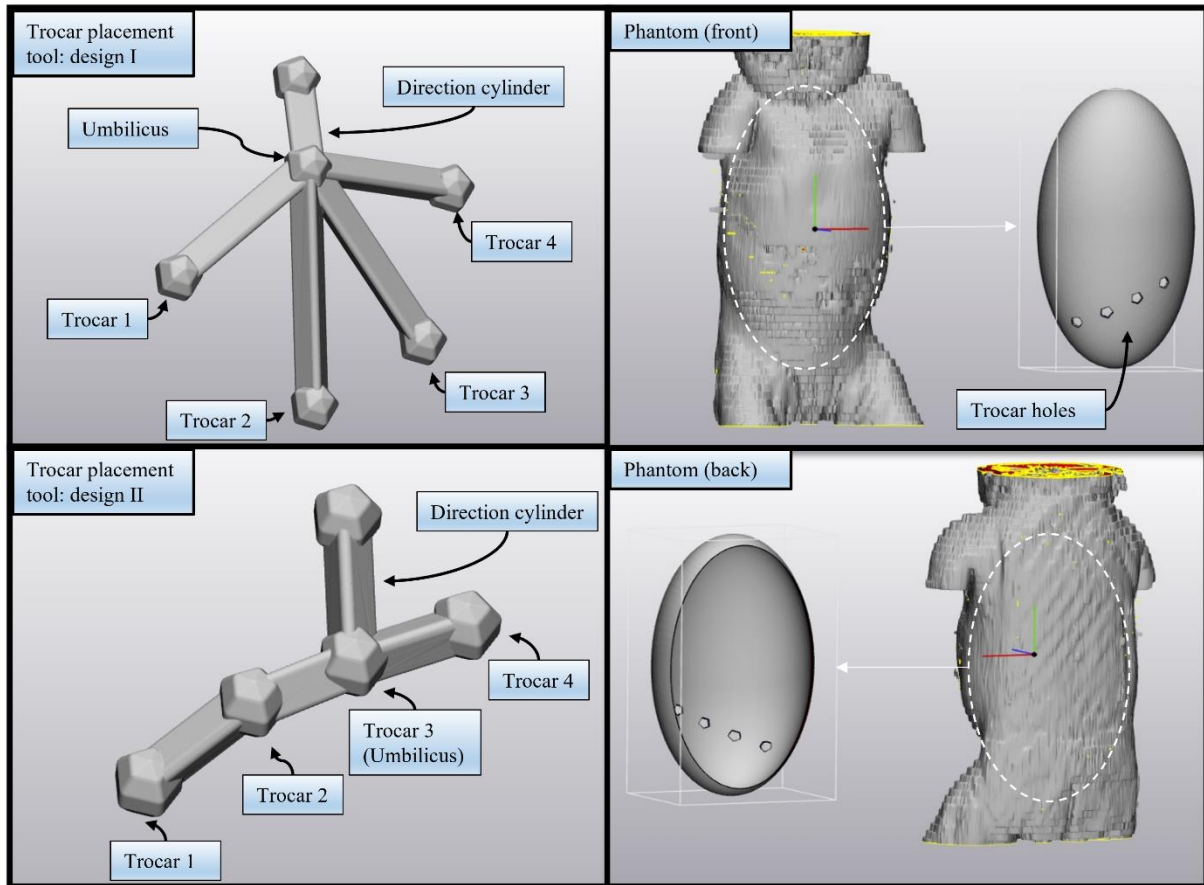


Fig. 10 Three-dimensional (3D) trocar placement tools and 3D phantom (right panel) of a young child's torso, designed in Materialise 3-Matic (Materialise, Leuven, Belgium). Left panel) Trocar placement tool design I was designed by four selected trocar locations with the trocar placement GUI, visualized as pentagon shapes. The pentagon shapes are connected by triangular prisms towards another pentagon shape, which represents the location of the umbilicus. A vertical cylinder is added to the umbilicus shape, to point out the direction of the tool during the usage. Trocar placement tool design II was designed similar, but in contrast with design I, the location of trocar 3 is identical to the umbilicus. Therefore, the connection triangular prisms were designed in between each pentagon shape. Right panel) Front and back view of the 3D phantom, based on the torso of the segmented child which is indicated by the white striped ellipsoid and arrow. The phantom contains holes representing the trocar locations selected in the GUI.

### 3.3 Trocar placement comparison

What follows is the comparison between the two different types of port placements. Fig. 9 shows the resulting figure after clicking button E in the results GUI, which is the occupied volume during the trajectory of the last external link. The left panel shows the result after the semicircular placement, the right panel shows the result of the straight-line trocar placement. A sketch of the trocar placements is shown in the bottom right corner of both figures.

The cone-shaped volumes are marked with the same color as the trocar for identification. The internal volumes are marked with a black edge color. The external volumes are also presented in  $m^3$  on top of the figures. As seen by Fig. 9 the semi-circular trocar placement causes more dispersion of the occupied volumes and therefore less overlapping. On the other hand, the overall occupied external volumes of the semi-circular trocar placement are less compared to the straight trocar line placement.

### 3.4 Trocar placement tool and phantom design

Fig. 10 shows the completion results in Materialise 3-Matic of the 3D trocar placement tool designs (left panel) and the 3D phantom (right panel) viewed from the front- and backside.

As shown by the left panel of Fig. 10, both designs consisted of pentagon shapes representing the chosen trocar locations of the GUI. In design I, the location of the umbilicus is added to know where the tool should be placed on the abdomen. This is in contrast with design II, where trocar 3 was located equal to the umbilicus. The pentagon shapes were connected by triangular prisms. In design I, these prisms are pointing towards the umbilicus shape, as in design II the pentagon shapes were connected one by one. Both designs have an additional vertical triangular prism on top of the umbilicus shape, to point out the direction of the tool during placement.

As indicated by the right panel of Fig. 10, the 3D phantom, shaped like an ellipsoid, was based on the measurements of the segmented torso

of a young child. The phantom contained holes, which were also located on the chosen trocar coordinates in the GUI. In addition, the backside of the ellipsoid was sliced off to create hollowness, as seen in the backside view.

The completion design protocol of the 3D trocar placement tool and phantom in Materialise 3-Matic is shown in Appendix C.

## 4. Discussion

This research provided an easy-to-use graphical tool with integrations of previous studies to compare the results of different trocar port placements. Therefore, this study gained more insight into the optimal positioning of robot arms inside the abdominal cavity in pediatric surgery. In addition, this research combined the graphical components with a clinical outlook, by the design of a 3D trocar placement tool and 3D phantom for future clinical validation.

### 4.1 Graphical user interfaces

Two GUIs were designed, the addition of the trocar placement GUI to the pipeline of previous studies about port optimization allowed the integration of the surgeon opinion [15]. It also gives the option to compare different trocar placements, like the ones researched in this study. Furthermore, by designing GUI II the surgeons only have to click a button to see any result of the kinematic robot model designed in previous research [15], [16]. This way surgeons need less technical knowledge, to have access to these results.

Unfortunately, there are limitations concerning the GUIs, especially regarding the patient model. A large drawback was that all figures in this research were based on the one manually designed surface patch model, based on the segmented young child provided by previous research [21], [22]. Other patient data was not considered in this research. Yet, this was the only available segmented infant patient data. In addition, for a more realistic approach, it would be better to use the segmented data instead of the surface patch. This decision was made to ease the connection between the patient model and the kinematic robot model. It also had the advantage that the surface patch smoothened the surface, and it drastically speeded up the GUI, compared to the large amount of segmented data. Nonetheless, another drawback to the patient model was that it did not include the pneumoperitoneum. Future research could easily solve this by incorporating a half ellipsoid on top of the model, as described in the study of Rademakers, (2020). The author also described how to automatically select the dimensions of the segmented abdomen by finding the maximum X, Y, Z coordinates. Such method should also be

incorporated in the GUI so that the patient surface patch will be automated designed in the future.

### 4.2 Kinematics

This research studied the comparison between the straight line and semi-circular line trocar placement. The kinematic results in terms of occupied external volumes of the arms did not show tremendous differences. The differences would have been perhaps larger if the coordinates between the trocar placements differed more. Though, the semi-circular trocars did contain more spreading of the external volumes, which could indicate less chance of collision. This advantage of the semi-circular line is in contrast to the golden standard of the da Vinci Xi clinical specialty guide and UMCG [9]. On the other hand, this was only based on the overlapping colors of the external volumes. Therefore, future research should implement a percentage of overlapping volumes of the robot arms to provide a more clear insight into the collision chance.

Furthermore, the unrealistic docking of the kinematic robot was improved by setting the range constraint, but further optimization of the robot is needed. Unfortunately, the GIK solver for the configurations of the last external link along the circular trajectory did not take the collision of the robotic arms with each other into account. Therefore, future research should implement collision chance indices that provide more kinematic information. Also, due to time constraints, the visualization of the robot was not adjusted. As stated in previous research, the dimensions do not go along with the kinematic model and therefore need further improvement [15].

### 4.3 3D trocar tool and phantom

The 3D trocar tool and phantom design seemed a promising setup for future clinical validation studies. However, the study is limited by the fact that both the trocar tool and phantom were not 3D printed, and therefore not validated due to time constraints. Nevertheless, both the trocar tool and phantom consisted of simple printed shapes that are easily changeable. The decision of choosing the pentagon and prims shapes for the trocar tool was to avoid overlapping triangles within the 3D object. The overlapping occurred when shapes with a higher number of triangles were implemented initially. This includes shapes such as spheres, which may look aesthetically pretty, but will cause too many mistakes for the 3D printing.

As seen in Fig. 10, two tool designs were made. A drawback due to time constraints was that the GUI was manually set to design either one of them. Therefore, it did not automatically choose what design should be produced based on the trocar locations. Future research could automate this

process by writing two m-scripts that each load in one of the designs, in which an extra GUI button is needed as well. The scripts also do not automatically recognize which of the trocar is located at the umbilicus and is now set on trocar 3. This could be solved in the future by finding the trocar with the closest distance to the umbilicus.

In terms of the phantom shape, the design consisted out of the abdominal ellipsoid of the surface patch. Therefore, the design came close to the sizes of the segmented young child as seen in Fig. 10. Thereby, using a simplified shape such as an ellipsoid as a base, future phantoms can easily be adjusted to any patient size. However, using a common printer like the Ultimaker S3 for fast prototype 3D printing, the size of the phantom could be too large compared to the printer [23]. Therefore, the protocol of Appendix C suggested that the phantom design can be sliced, for example in half. If slicing is needed, future studies should implement a connective construction that allows the phantom parts to be hooked within each other. A suggestion would be to add some sort of cantilever snap joint to the design [24]. A drawback of the phantom design was that only the outer part of the child's torso was considered. For a more realistic approach, it is recommended that the target organ, as well as important surrounding structures, are extracted out of MRI/CT data and 3D fabricated as well, like in the study of Heunis et al. (2020) [25]. Finally, both the 3D trocar tool and phantom were given a thickness of 3mm. This thickness was chosen due to providing a balance between strength, material savings, and costs, which was previously studied in 3D printed mold studies [26], [27].

#### *4.4 Future research*

Although this research contributed to the research pipeline for port optimization in pediatric robotic surgery, more research is needed to clinically validate the kinematic models before future implementation. The designed 3D trocar tool and phantom need to be printed, validated, and optimized to be used for clinical validation studies. The design protocols of this research can be used as

a base to design tools and phantoms for any type of pediatric patient. For the implementation of other pediatric patients, the GUI needs to be optimized to fully extract the dimensions of the patient's torso for the design of the surface patch model where the phantom was designed from. In addition, future research should implement segmented internal organs to the phantom that are critical structures for pediatric choledochal malformation surgery. In terms of the trocar placement tool, future research should further improve the GUI to automatically select which trocar placement tool design needs to be created based on the chosen trocar coordinates.

Furthermore, although the docking procedure was improved in this research, future research should further improve the kinematic robot model. The collision between the robotic arms during the trajectory configuration should be implemented in terms of collision change indices. This will provide more clear kinematic information that can be compared for different port placements. Also, the dimensions and ratios of the 3D visualization of the robot should be further researched to go along with the kinematic robot model.

## **5. Conclusion**

This research designed an easy-to-use trocar placement GUI to optimize the port placement in pediatric abdominal surgery. The GUI combines the surgical decision-making in trocar placement by integration of GIK solvers of previous port optimization studies, to calculate the docking, robot arm research, and collision of a kinematic robot model for different trocar placements. In addition, a second GUI was designed to have a quick and easy visualization of the kinematic robot results. Future research is needed to optimize the kinematic model and to provide more insight into the collision between the robot arms. This research also used the GUIs to design 3D printed trocar placement tools and the phantom that can be used as a setup for future clinical validation studies. These studies are necessary to validate the kinematic model and safely gain further insight into port optimization.

## REFERENCES

- [1] S. Dawda, M. Camara, P. Pratt, J. Vale, A. Darzi, and E. Mayer, "Patient-Specific Simulation of Pneumoperitoneum for Laparoscopic Surgical Planning," *J. Med. Syst.*, vol. 43, no. 10, 2019, doi: 10.1007/s10916-019-1441-z.
- [2] F. Köckerling, "Robotic vs. Standard Laparoscopic Technique – What is Better?," *Front. Surg.*, vol. 1, no. May, pp. 10–13, 2014, doi: 10.3389/fsurg.2014.00015.
- [3] J. M. Ferguson *et al.*, "Comparing the accuracy of the da Vinci Xi and da Vinci Si for image guidance and automation," *Int. J. Med. Robot. Comput. Assist. Surg.*, vol. 16, no. 6, pp. 1–10, 2020, doi: 10.1002/rcs.2149.
- [4] N. K. Alizai, M. J. Dawrant, and A. S. Najmaldin, "Robot-assisted resection of choledochal cysts and hepaticojejunostomy in children," *Pediatr. Surg. Int.*, vol. 30, no. 3, pp. 291–294, 2014, doi: 10.1007/s00383-013-3459-5.
- [5] K. R. Sheth and C. J. Koh, "The Future of Robotic Surgery in Pediatric Urology: Upcoming Technology and Evolution Within the Field," *Front. Pediatr.*, vol. 0, no. JULY, p. 259, Jul. 2019, doi: 10.3389/FPED.2019.00259.
- [6] K. C. Soares *et al.*, "Pediatric choledochal cysts: diagnosis and current management," *Pediatr. Surg. Int.*, vol. 33, pp. 637–650, 2017, doi: 10.1007/s00383-017-4083-6.
- [7] R. H. De Kleine, A. Ten Hove, and J. B. F. Hulscher, "Long-term morbidity and follow-up after choledochal malformation surgery; A plea for a quality of life study ☆," *Semin. Pediatr. Surg.*, vol. 29, p. 150942, 2020, doi: 10.1016/j.sempedsurg.2020.150942.
- [8] L. W. Sun and C. K. Yeung, "Port placement and pose selection of the Da Vinci surgical system for collision-free intervention based on performance optimization," *IEEE Int. Conf. Intell. Robot. Syst.*, pp. 1951–1956, 2007, doi: 10.1109/IROS.2007.4399354.
- [9] R. G. Stricko, B. Page, A. E. Kerdok, B. Itkowitz, and J. Pile, "Port placement optimization for robotically-assisted minimally invasive surgery," *Front. Biomed. Devices, BIOMED - 2018 Des. Med. Devices Conf. DMD 2018*, pp. 1–4, 2018, doi: 10.1115/DMD2018-6840.
- [10] G. Pelizzo *et al.*, "Pediatric Laparoscopy and Adaptive Oxygenation and Hemodynamic Changes," *Pediatr. Rep.*, vol. 9, no. 2, pp. 21–25, 2017, doi: 10.4081/PR.2017.7214.
- [11] E. Trovalusci, M. Gasparella, C. Pizzato, and P. Midrio, "The Alexis® system for laparoscopic splenectomy in pediatric patients," *Updat. Surg. 2021*, vol. 1, pp. 1–5, Apr. 2021, doi: 10.1007/S13304-021-01023-5.
- [12] J. A. Zaman and T. P. Singh, "The emerging role for robotics in cholecystectomy: the dawn of a new era?," *HepatoBiliary Surg. Nutr.*, vol. 7, no. 1, pp. 21–28, Feb. 2018, doi: 10.21037/hbsn.2017.03.01.
- [13] S. A. Yeo *et al.*, "Universal suprapubic approach for complete mesocolic excision and central vascular ligation using the da Vinci Xi® system: from cadaveric models to clinical cases," *J. Robot. Surg.*, vol. 11, no. 4, pp. 399–407, Dec. 2017, doi: 10.1007/s11701-016-0664-y.
- [14] M. Kim *et al.*, "A development of assistant surgical robot system based on surgical-operation-by-wire and hands-on-throttle-and-stick," *Biomed. Eng. Online*, vol. 15, no. 1, May 2016, doi: 10.1186/s12938-016-0189-7.
- [15] C. W. A. Pruijssers, "Optimal positioning of robot arms inside the abdominal cavity , to achieve optimal sight and range of motion in pediatric

- surgery Research report clinical internship III University of Twente,” 2021.
- [16] E. Bock de, “Optimisation of port placement in paediatric robot-assisted laparoscopic surgery using the da Vinci Xi,” 2021.
- [17] “The da Vinci® system: technology and surgical analysis | Ento Key,” 2019. <https://entokey.com/the-da-vinci-system-technology-and-surgical-analysis/> (accessed Jun. 03, 2021).
- [18] J. M. Xu *et al.*, “Robot-assisted one-stage resection of rectal cancer with liver and lung metastases,” *World J. Gastroenterol.*, vol. 21, no. 9, pp. 2848–2853, Mar. 2015, doi: 10.3748/wjg.v21.i9.2848.
- [19] A. Renfrew, “Book Review: Introduction to Robotics: Mechanics and Control,” *Int. J. Electr. Eng. Educ.*, vol. 41, no. 4, pp. 388–388, 2004, doi: 10.7227/ijeee.41.4.11.
- [20] TekkotsuRobotics, “Denavit-Hartenberg Reference Frame Layout - YouTube,” 2009. <https://www.youtube.com/watch?v=rA9tm0gTln8>.
- [21] F. Rademaker, “Optimal Positioning of Robotic Arms in Pediatric Robotic Surgery : a Trocar Placement Model ( concept ),” 2020.
- [22] P. de Graaf, “Optimal Positioning of Robotic Arms Inside the Abdominal Cavity in Pediatric Surgery,” pp. 0–20, 2020.
- [23] Green Field Chemtech, “Technical Data Sheet TPU G1095AU-B,” no. 2, pp. 9–11, 2018.
- [24] S. Doltsinis, M. Krestenitis, and Z. Doulgeri, “A Machine Learning Framework for Real-Time Identification of Successful Snap-Fit Assemblies,” *Trans. Autom. Sci. Eng.*, vol. 17, no. 1, pp. 513–523, 2020, doi: 10.1109/TASE.2019.2932834.
- [25] C. M. Heunis, Y. P. Wotte, J. Sikorski, G. P. Furtado, and S. Misra, “The ARMM System - Autonomous Steering of Magnetically-Actuated Catheters: Towards Endovascular Applications,” *IEEE Robot. Autom. Lett.*, vol. 5, no. 2, pp. 704–711, 2020, doi: 10.1109/LRA.2020.2965077.
- [26] A. Ooms, “Implementation of sterilized 3D -printed breast molds for autologous breast reconstructions,” pp. 1–61, 2021.
- [27] J. B. Troost, “Usability study to obtain design and manufacturing recommendations for the optimal 3D printed mold for autologous breast reconstruction,” p. 35, 2020.



## Appendix A: Trocar placement GUI

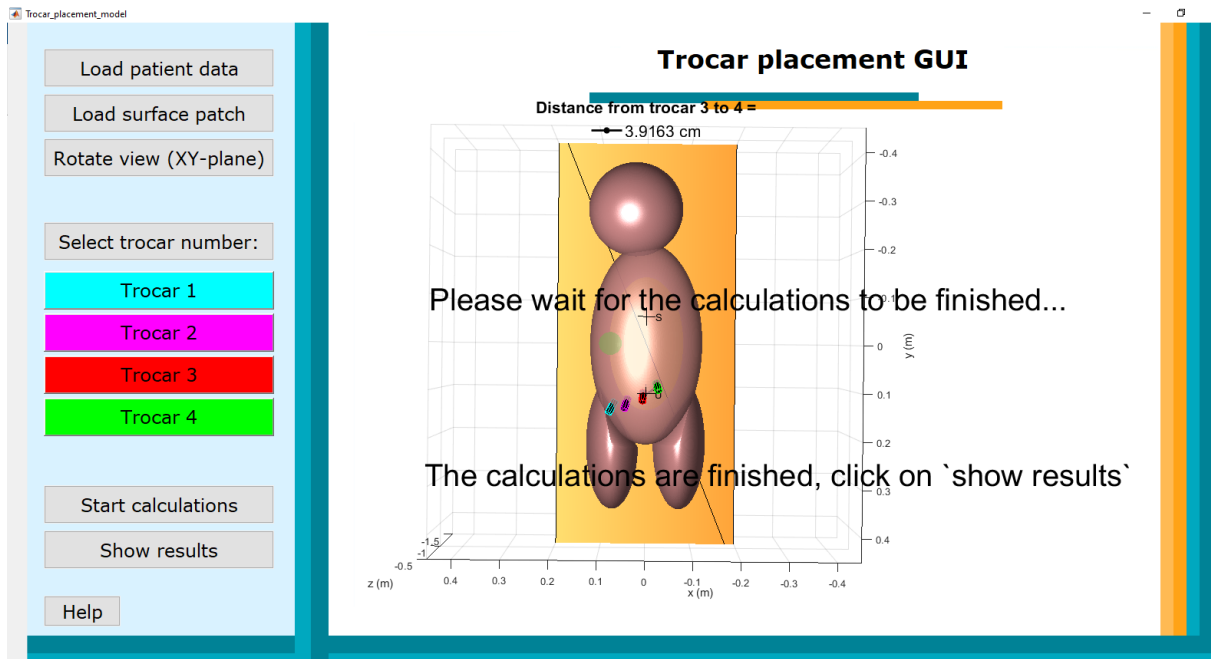


Fig. 11. Trocar placement graphical user interface (GUI) waiting screen. The 'Please wait..' text appears after the 'start calculations' button is clicked. After finishing the calculations, the other text line appears which informs the user that the 'show results' button is allowed to be pressed.

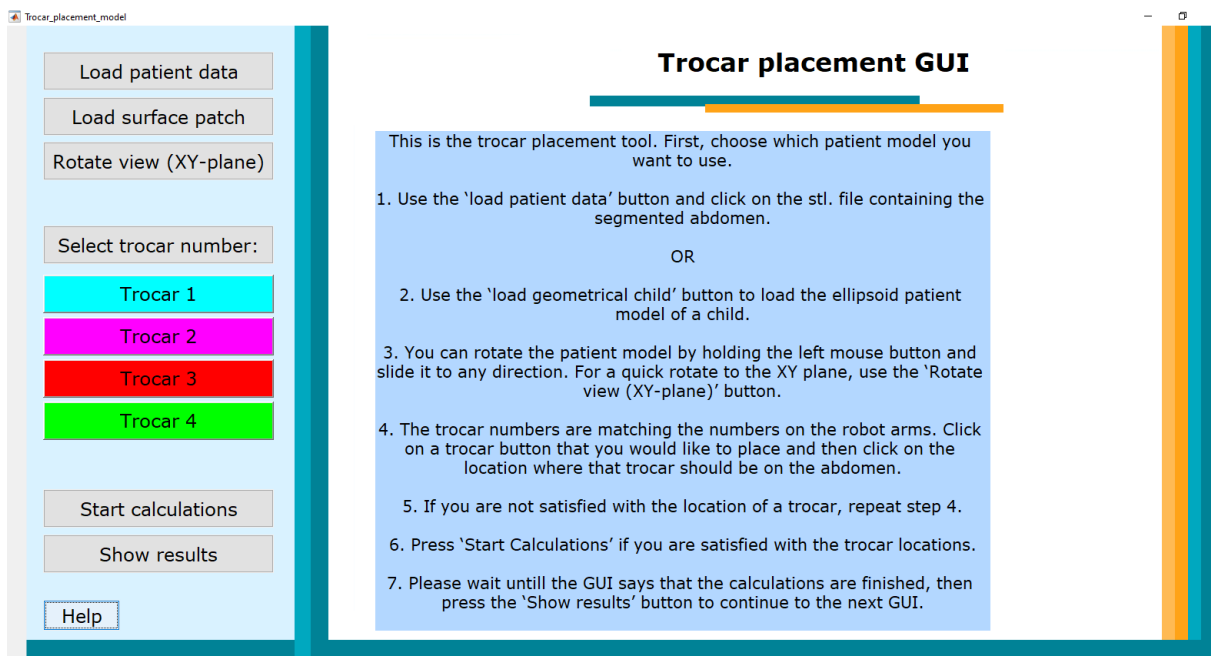


Fig. 11. Trocar placement graphical user interface (GUI) help text screen. The help text appears after clicking the 'help' button, it disappears after clicking it again.

## Appendix B: Results GUI

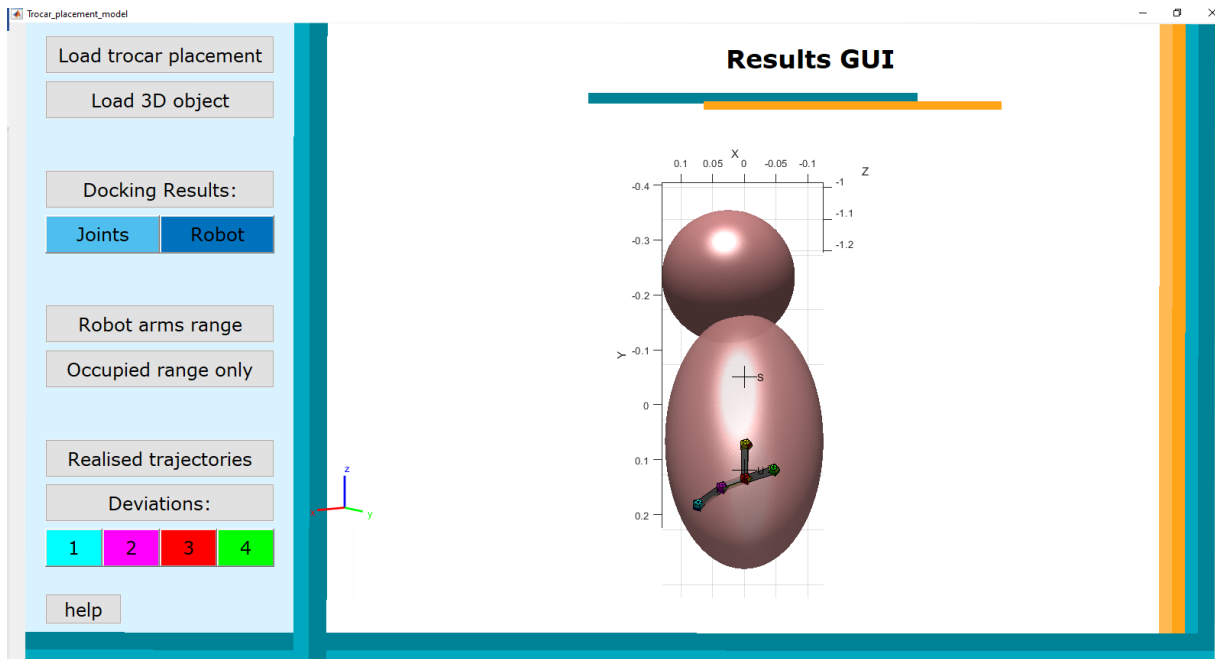


Fig. 12 Screen of the results Graphical User Interface (GUI) in MATLAB (2021a) showing the graphic 3D trocar placement tool design. The design consists of four heptagons at the coordinates of the trocar placement of the trocar placement GUI, connected by triangular prisms. At the third trocar which is located at the umbilicus, a vertical prism is added to point out the direction during the use of the tool.

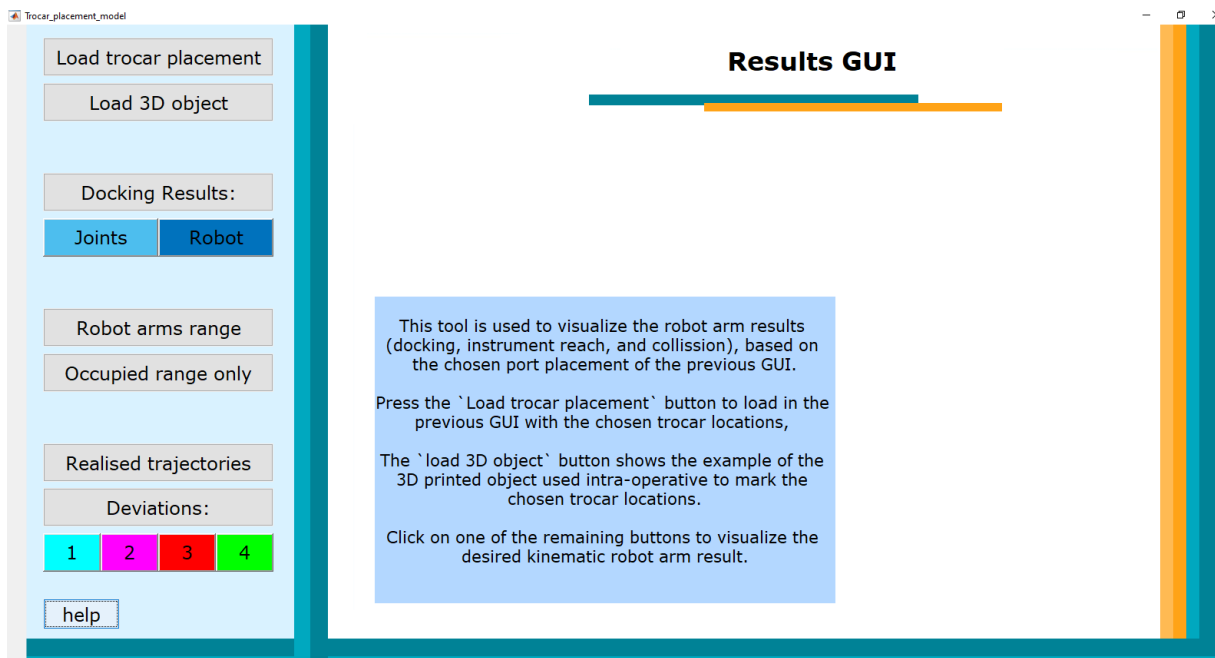


Fig. 134. Trocar placement graphical user interface (GUI) help text screen. The help text appears after clicking the 'help' button, it disappears after clicking it again.

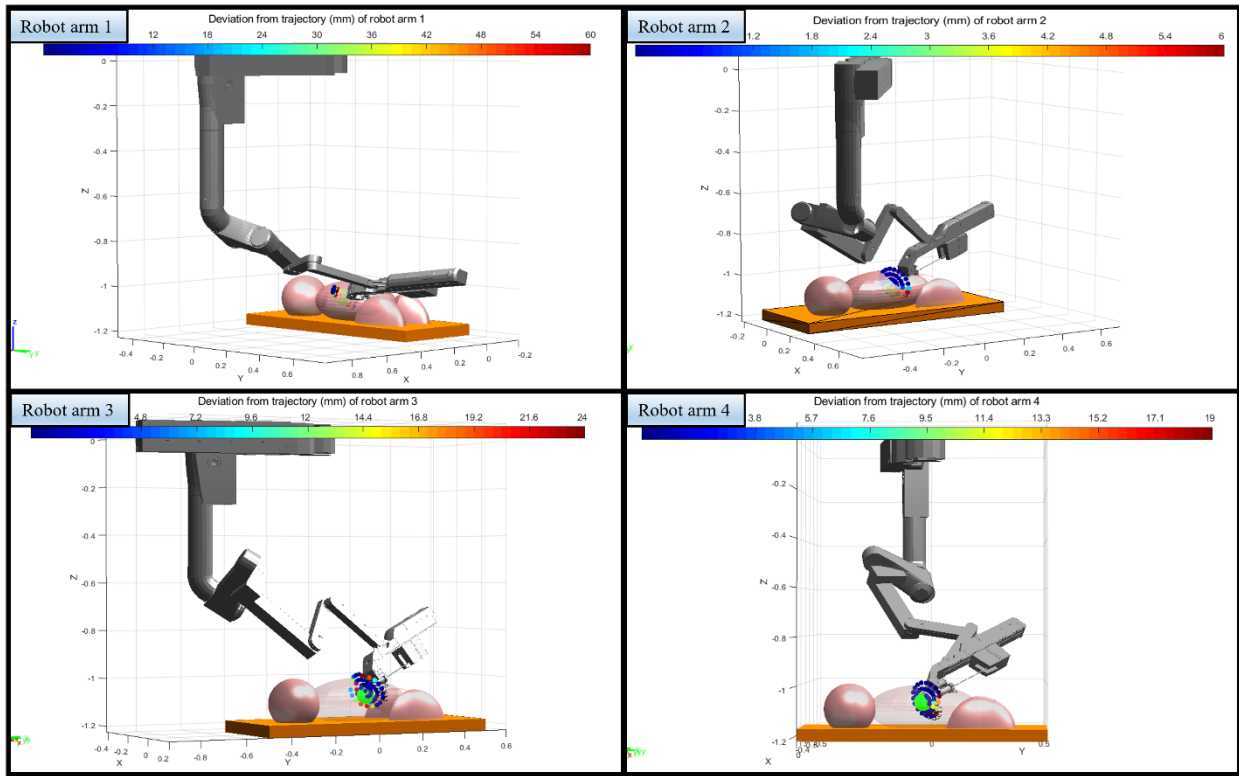


Fig. 14. Deviation from the realized trajectories of the four robot arms for the straight-line trocar placement. The colorbar indicates how much the position of the tool deviates of the planned trajectory in millimeters. The 'c' indicates where the arm collided with the patient or table. Note that robot arm 1 has the most trajectory deviation and robot arm 2 the least. Both robot arms 3 and 4 have collision as indicated by the 'c'.


## Appendix C: Completion 3D trocar placement tool and phantom

### Deel I: Fantoom model


#### 1. Voorbereiden 3D-object in MATLAB

Allereerst moet het 3D object worden ingeladen in Materialise 3-Matic. Zorg ervoor dat het 3D-object als STL-bestand heeft opgeslagen op de computer waarop u werkt. Zorg er verder voor dat 3-Matic is geïnstalleerd op de computer en klaar is voor gebruik.

#### 2. Importeren van een 3D object


-  Links ziet u een verticale werkbalk met verschillende icoontjes. Klik op het icoon wat hoort bij *Import part*
- Selecteer de STL-bestanden die u wilt gebruiken. Dit is dus de abdomenmesh, en de betreffende trocar ellipsoïds.
- Een venster wordt geopend. Alle standaard instellingen zijn hierbij goed. Belangrijk is dat *Scale coefficient* op *mm* staat
- Druk op OK
- U ziet nu uw 3D model, deze is ook te vinden aan de rechterkant van uw scherm in de *Object Tree*.
- U kunt de objecten een nieuwe naam geven door dubbel te klikken op het object in de *Object Tree*

#### 3. Transleren van een 3D object

- Ga naar het tabblad *align*, te vinden in het blauw in de tweede horizontale balk
-  Klik op het icoon wat hoort bij *Interactive translate*. U ziet nu rechtsonder *Operations* het tabblad *Interactive translate* verschijnen
- Selecteer in Main entity het STL-object (grijs) en schuif deze aan de voorkant over het gekleurde OBJ door aan de pijlen te trekken.

#### 4. Schalen van een 3D object

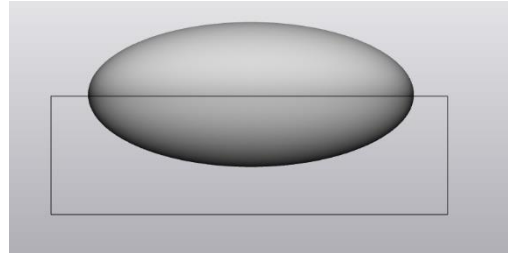
Om het 3D object de juiste schaal te geven, moet het object vergroot worden van mm-> m.

- Ga naar het tabblad *align*, te vinden in het blauw in de tweede horizontale balk
-  Klik op het icoon wat hoort bij *Scale*. U ziet nu rechtsonder *Operations* het tabblad *Scale* verschijnen
- Selecteer de STL-bestanden als *Entities* en zet de *Scale factor* op 1000. Zorg dat 'Uniform' aangevinkt is. Klik op *Apply*.

## 5. Fantoom verdelen in meerdere oppervlakten


Als u het fantoom uit bijvoorbeeld twee delen wilt maken, of bijvoorbeeld enkel de bovenste helft wilt gebruiken volg dan deze stappen.

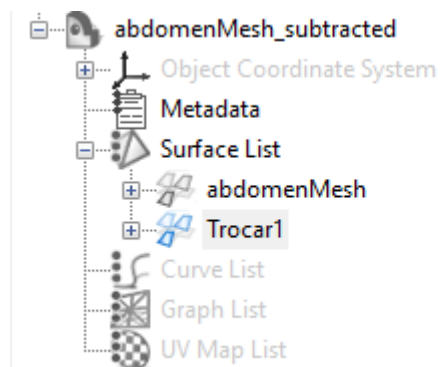
1. Ga naar het tabblad *Surface*, te vinden in het blauw in de tweede horizontale balk
2.  Klik op het icoon wat hoort bij *Rectangular Patch*. U ziet nu rechtsonder *Operations* het tabblad *Rectangular Patch* verschijnen. Zorg dat *All visible parts* en *Split through* aan staan.
3. Zorg ervoor dat u recht tegen het fantoom aankijkt. Dit kunt u doen door uw *default view* in uw gewenste richting te zetten.
4. Sleep uw vierkant over de gewenste richting van uw fantoom. U ziet nu een lijn verschijnen die het fantoom in tweeën heeft gesplitst.
5. Ga naar de *Object Tree* -> uw *Fantoom* -> *Surface List* -> klik op het betreffende oppervlak die u niet wilt gebruiken door met uw rechtermuis op *hide* te drukken. Of als uw deze wilt verwijderen, klik op *delete*.




## 6. Trocar gaten maken in het fantoom

Om de gaten in het fantoom te maken worden de trocar ellipsoiden afgetrokken van het fantoom model.

1. Ga naar het tabblad *Design*, te vinden in het rood in de tweede horizontale balk
2.  Klik op het icoon wat hoort bij *Boolean Subtraction*. U ziet nu rechtsonder *Operations* het tabblad *Boolean Subtraction* verschijnen
3. Selecteer als *Entities* uw abdomen mesh en als *Subtraction entities* uw trocar ellipsoiden. Klik op *Apply*.
4. De abdomen mesh heeft nu een ingedeukt oppervlakte op de locatie van de trocar. Verwijder dit ingedeukte oppervlak om een gat in uw fantoom te krijgen. Ga naar de *Object Tree* -> uw *Fantoom* -> *Surface List* -> klik op het betreffende oppervlak, en klik op *delete*.



## 7. Dikte geven aan het fantoom


1. Ga naar het tabblad *Design*, te vinden in het rood in de tweede horizontale werkbalk
2.  Klik op het icoon wat hoort bij *Uniform offset*. In de rechthoek van uw scherm, onder het kopje *Operations*, ziet u nu het tabblad *Uniform Offset*
3. Klik hier op *Entities* en selecteer uw object. De naam van dit object is nu zichtbaar bij *Entities*
4. Zorg ervoor dat bij de *Offset parameters*:
  - *Direction* op *External offset* staat
  - *Distance* op de gewenste dikte staat. 3 mm is een goede dikte voor een fantoom
  - *Preserve sharp features* uit staat
  - *Solid* aangevinkt is
5. Klik op *Apply*.



## Deel II: 3D trocar tool

Begin met het herhalen van stap 1 tot en met 4 van het fantoom model protocol. Laad de losse STL files in die alle onderdelen van de tool bevatten.

### 1. Verbinden van de losse onderdelen

6. Ga naar het tabblad *Design*, te vinden in het rood in de tweede horizontale werkbalk
7.  Klik op het icoon wat hoort bij *Boolean Union*. In de rechthoek van uw scherm, onder het kopje *Operations*, ziet u nu het tabblad *Boolean Union*
8. Klik hier op *Entities* en selecteer alle object die horen bij uw trocar tool. De namen van deze objecten zijn zichtbaar bij *Entities*
9. Klik op *Apply*.

## Deel III: Einde

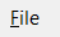
### Controleren op fouten



Klik nu op de *Fix Wizard*, te vinden bij het tabblad *Fix*. Er verschijnt een pop-up venter

1. Selecteer als *Part* het hele object wat bij uw trocar tool hoort
2. Zorg ervoor dat het vinkje *Full analysis* aanstaat
3. In het geel kunt u het advies vinden, hoe u het object het beste kan verbeteren. Door op het knopje *Follow Advice* te klikken, volgt hij automatisch zijn eigen advies op. U moet meerdere malen op dit knopje klikken, ideaal gezien tot alle getallen groen zijn
4. Blijf tijdens het doorklikken goed uw tool in de gaten houden. In principe moet het goed gaan, maar soms lost het programma fouten op de verkeerde manier op
5. Waarschijnlijk zullen er altijd wat *Overlapping triangles* of andere fouten blijven. Zolang dit er niet heel veel zijn is dit geen probleem

### Object exporteren als STL-bestand

1.  Selecteer in de eerste horizontale werkbalk *File* → *Export* → *STL*
2. Selecteer als *Entities* het object waar uw 3D object uit bestaat. Bij *Output directory* ziet u in welke map het bestand wordt opgeslagen
3. Klik op *Apply*. U heeft nu uw mal opgeslagen als STL-bestand. Deze kunt u nu importeren in de software die hoort bij uw 3D printer